



CHORUS

This is the accepted manuscript made available via CHORUS. The article has been published as:

High antiferromagnetic transition temperature of the honeycomb compound $\text{SrRu}_{2}\text{O}_{6}$

W. Tian, C. Svoboda, M. Ochi, M. Matsuda, H. B. Cao, J.-G. Cheng, B. C. Sales, D. G. Mandrus, R. Arita, N. Trivedi, and J.-Q. Yan

Phys. Rev. B **92**, 100404 — Published 14 September 2015

DOI: [10.1103/PhysRevB.92.100404](https://doi.org/10.1103/PhysRevB.92.100404)

High antiferromagnetic transition temperature of a honeycomb compound SrRu₂O₆

W. Tian,¹ C. Svoboda,² M. Ochi,³ M. Matsuda,¹ H. B. Cao,¹ J.-G. Cheng,⁴
B. C. Sales,⁵ D. G. Mandrus,^{5,6} R. Arita,³ N. Trivedi,² and J.-Q. Yan^{5,6}

¹Quantum Condensed Matter Division, Oak Ridge National Laboratory, Oak Ridge, Tennessee 37831, USA

²Department of Physics, The Ohio State University, Columbus, Ohio 43210, USA

³RIKEN Center for Emergent Matter Science, 2-1 Hirosawa, Wako, Saitama 351-0198, Japan

⁴Beijing National Laboratory for Condensed Matter Physics, and Institute of Physics,
Chinese Academy of Sciences, Beijing 100190, P. R. China

⁵Materials Science and Technology Division, Oak Ridge National Laboratory, Oak Ridge, Tennessee 37831, USA

⁶Department of Materials Science and Engineering,
University of Tennessee, Knoxville, Tennessee 37996, USA

(Dated: August 10, 2015)

We study the high temperature magnetic order in a quasi-two-dimensional honeycomb compound SrRu₂O₆ by measuring magnetization and neutron powder diffraction with both polarized and unpolarized neutrons. SrRu₂O₆ crystallizes into the hexagonal lead antimonate (PbSb₂O₆, space group $P\bar{3}1m$) structure with layers of edge-sharing RuO₆ octahedra separated by Sr²⁺ ions. SrRu₂O₆ is found to order at $T_N=565$ K with Ru moments coupled antiferromagnetically both in-plane and out-of-plane. The magnetic moment is 1.30(2) μ_B /Ru at room temperature and is along the crystallographic c -axis in the G-type magnetic structure. We perform density functional calculations with constrained RPA to obtain the electronic structure and effective intra- and inter-orbital interaction parameters. The projected density of states show strong hybridization between Ru $4d$ and O $2p$. By downfolding to the target t_{2g} bands we extract the effective magnetic Hamiltonian and perform Monte Carlo simulations to determine the transition temperature as a function of inter- and intra-plane couplings. We find a weak inter-plane coupling, 3% of the strong intra-plane coupling, permits three-dimensional magnetic order at the observed T_N .

PACS numbers: 75.50.Ee, 75.47.Lx, 75.30.Et, 71.15.Mb,

It is evident that for the design of the next generation of multifunctional devices, we need new paradigms, new principles and new classes of materials. Magnetism is arguably the most technologically important property arising from electron interactions. One of the central questions has been how to create magnetic materials with high transition temperatures T_c for room temperature devices. Broadly two paradigms define the formation of the magnetic state starting with fermions at finite temperatures: for weak Coulomb interactions U/W compared to the bandwidth, one expects a Fermi liquid at finite temperatures, followed by a Fermi surface nesting instability that opens a gap in the spectrum resulting in a Slater antiferromagnet below $T_c \sim W e^{-c\sqrt{W/U}}$ which is exponentially suppressed in the coupling (c is a constant). In the opposite regime for $U/W \gg 1$, local moments form on a much higher temperature scale $T^* \approx U$ opening a large Mott gap and order on the scale of antiferromagnetic (AF) superexchange $J \sim W^2/U$. The transition temperature as a function of U/W reaches its maximum in the fluctuating regime with $U \approx W$. SrTcO₃ is currently believed to be at the maximum with a $T_c \approx 1000$ K [1–6]. Tuning U/W by combining different $3d$ and $5d$ ions in double perovskites also increases T_c well above room temperature [7], as in Sr₂CrReO₆ with a $T_c = 635$ K [8] and in Sr₂CrOsO₆ with a $T_c = 720$ K [9]. These are examples of Mott-Hubbard antiferromagnetic insulators. NaOsO₃ orders at $T_c = 410$ K [10, 11], which is a rare example of

Slater insulator approaching the fluctuating region from the itinerant side. All the above reported high T_c compounds have perovskite structures with a d^3 electronic configuration. Experimental studies of these interesting osmates and technetium compounds have been impeded by the safety concerns from toxic osmium oxide (mainly OsO₄) and radioactive technetium.

Recently, a metastable compound SrRu₂O₆ with a quasi-two-dimensional structure was proposed to order antiferromagnetically with T_N above 500 K [12]. SrRu₂O₆ crystallizes into the hexagonal lead antimonate (PbSb₂O₆) structure with the space group $P\bar{3}1m$. As shown in the inset of Fig. 1, the structure consists of layers of edge-sharing RuO₆ octahedra separated by Sr²⁺ ions sitting in the oxygen octahedral interstices. In the ab plane, the Ru ions form a honeycomb array. In the previous study [12], the magnetization was measured up to 500 K without finding a signature for the magnetic transition, though the room temperature neutron powder diffraction observed extra reflections absent in x-ray measurements.

In this Letter, we report our magnetic and neutron diffraction study of SrRu₂O₆ up to 750 K. Our diffraction measurements with both polarized and unpolarized neutrons confirm that SrRu₂O₆ orders antiferromagnetically at $T_N = 565$ K with a magnetic moment of 1.30(2) μ_B /Ru along c -axis. The magnetic measurements suggest that strong two-dimensional magnetic cor-

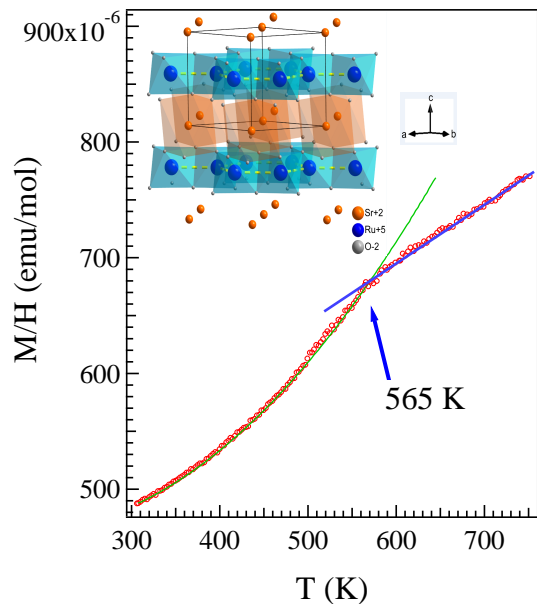


FIG. 1. (color online) Magnetic susceptibility in the temperature range $300 \text{ K} \leq T \leq 750 \text{ K}$ measured upon cooling in an applied field of 50 kOe. The solid curves highlight the slope change at 565 K. Inset shows the crystal structure.

relations persist above T_N as highlighted in Fig. 1 above the kink. We discuss below band structure calculations that show strong Ru 4d and O 2p hybridization, the role of different exchange pathways, and the derivation of an effective model with in-plane and inter-plane magnetic interactions, to explain the mechanisms and high ordering temperature of SrRu_2O_6 .

We synthesize polycrystalline SrRu_2O_6 by a hydrothermal technique as reported previously [12]. Fig. 1 shows the temperature dependence of magnetic susceptibility measured in the temperature range $300 \text{ K} \leq T \leq 750 \text{ K}$ using a Quantum Design magnetic property measurement system. The data collected in warming and cooling processes overlap suggesting little or no sample decomposition below 750 K. Above room temperature, the magnetic susceptibility increases with increasing temperature. As highlighted by the solid curves, there is a slope change at 565 K, which signals possible long range magnetic order.

To study the nature of this slope change, we carry out neutron diffraction experiments in the temperature range $40 \text{ K} \leq T \leq 600 \text{ K}$. [13] As shown in Fig. 2(a), neutron powder diffraction observed reflections that are absent in x-ray powder diffraction pattern. To confirm the magnetic origin of these extra reflections, we perform diffraction measurement using polarized neutrons. With the spin flipper off or on, we measured both the $(++)$ non-spin-flip and the $(-+)$ spin-flip scattering of $(1\ 0\ 0.5)$ and $(1\ 0\ 1)$, respectively (Fig. 2(b) and (c)). As discussed in Refs. [13–16], the strong scattering detected in the $(-+)$

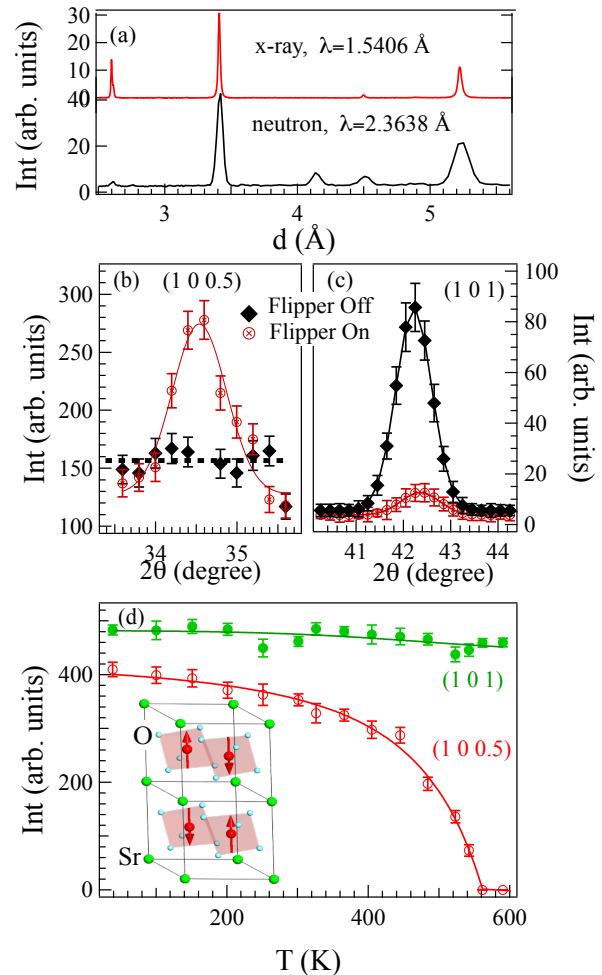


FIG. 2. (color online) (a) Room temperature x-ray and neutron powder diffraction patterns in a narrow d -range highlighting the extra reflections observed by neutron diffraction. (b) and (c) show the $(1\ 0\ 0.5)$ magnetic and $(1\ 0\ 1)$ nuclear peaks measured with the polarized neutron in the horizontal field configuration $P_0 \parallel Q$ at room temperature, respectively. The observed weak intensity in (c) with flipper on comes from the finite instrumental flipping ratio which we estimate to be 1/10 by comparing the integrated intensity of the $(-+)$ and $(++)$ scans of $(1\ 0\ 1)$. (d) The temperature dependence of integrated intensity of $(1\ 0\ 0.5)$ and $(1\ 0\ 1)$ peaks. The solid curves are a guide to the eye. Inset shows the G-type magnetic structure.

spin-flip channel confirmed the magnetic origin of the $(1\ 0\ 0.5)$ peak.

The diffraction study with polarized neutrons clearly shows that the extra reflections come from a long range magnetic order instead of any structural transition. Those extra reflections can be indexed on the basis of the magnetic scattering with a G-type AF structure with the magnetic moment direction along the crystallographic c -axis. The Rietveld refinement of the neutron diffraction patterns [13] yields a magnetic moment of $1.30(2)$

μ_B/Ru at 300 K. The magnetic moment increases slightly to $1.34(3) \mu_B/\text{Ru}$ upon cooling to 40 K. The moment is smaller than the spin moment of $3 \mu_B$ expected for a half-filled t_{2g} band, which signals a strong covalency of the Ru-O bonds.

As shown in Fig. 2(d), the (1 0 0.5) magnetic peak disappears around 565 K, where a slope change is observed in Fig. 1 in the temperature dependence of the magnetic susceptibility. Figure 2(d) also shows the evolution with temperature of the integrated intensity of the (1 0 1) nuclear peak, which shows little temperature dependence. The coincidence of the disappearance of (1 0 0.5) magnetic peak and the slope change in magnetic susceptibility suggests that a G-type long range magnetic order takes place at 565 K in SrRu_2O_6 .

In SrRu_2O_6 the Ru ions are in a d^3 electronic configuration in edge-shared octahedral cages formed by the O atoms. In the presence of correlations, we expect this half-filled system in the t_{2g} manifold to be a Mott insulator. It is important to note that the Ru-O-Ru bond angle is close to 90° hence both ferromagnetic (F) and AF mechanisms through intermediate oxygens are active in fourth order processes according to Goodenough-Kanamori rules [17, 18]. There are three competing processes that contribute to the exchange interaction: (a) the direct overlap of the half filled t_{2g} orbitals produces a second order AF interaction. (b) The transfer of electrons between an oxygen p_z orbital and Ru d_{zx} and d_{yz} orbitals on two neighboring Ru atoms results in an AF superexchange coupling. (c) The transfer of electrons between Ru t_{2g} orbitals and mutually orthogonal oxygen p orbitals results in a F interaction driven by Hund's coupling on oxygen.

It is rather intriguing that SrRu_2O_6 orders at such a high temperature, given the competing magnetic interactions. To estimate the relative magnitude of the above competing interactions and to understand the mechanism for the high AF ordering temperature, we perform DFT calculations including constrained RPA to obtain effective hopping and interaction parameters. We also perform spin density functional calculation with the WIEN2K [19] package using the exchange-correlation functional proposed by Perdew *et al.* [20] and the full-potential linearized augmented plane-wave method including the spin-orbit coupling. In the calculation, we use the experimental lattice parameters and atomic configurations determined at room temperature [12].

Our DFT calculation shows that the G-type AF state is the most stable. The non-magnetic (NM) and the C-type AF (i.e., AF in the ab -plane and F along the c -axis) states have higher energy than that for the G-type AF state, and there is no ferromagnetic or A-type AF (i.e., F in the ab -plane and AF along the c -axis) metastable solution. These results indicate that there is a strong in-plane AF correlation compared with that for the out-of-plane direction. Calculated local spin magnetic moment

of Ru atoms is about $0.9 \mu_B$ per atom for the G-type AF state and in reasonable agreement with our experiment. Fig. 3 shows the band dispersion and (projected) density of states (DOS) for the NM state. The t_{2g} bands [24] are well isolated from the e_g and oxygen p bands. Strong Ru-O hybridization is seen in the DOS, which points to the origin of the reduced local spin magnetic moment of Ru atoms. Possible quantum fluctuations arising from the quasi-two dimensional structure and orbital fluctuations may also suppress the magnetic moment; but their contribution should be small. The band dispersions of the NM and AF phases are very similar; The NM state has a small band gap of 0.05 eV, which increases to 0.14 eV in the G-type AF state.[13]. We have measured the temperature-dependent resistivity $\rho(T)$ on a dense pellet [13]. The material is insulating with an activated gap of 0.036 eV. The reduced gap compared to LSDA can arise due to the presence of disorder induced localized states in the sample.

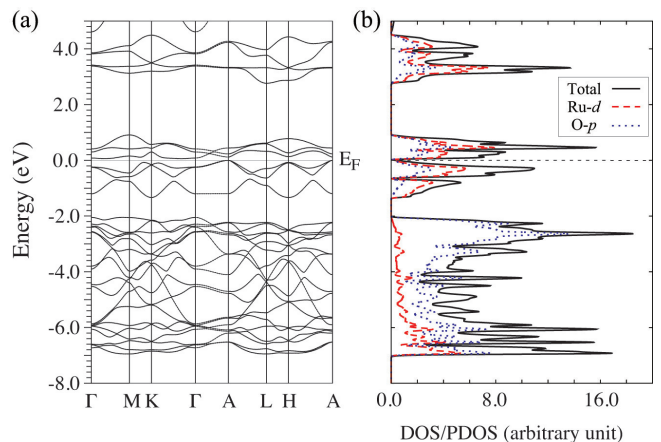


FIG. 3. (color online): (a) Band dispersion and (b) (projected) density of states for the non-magnetic state.

Using a density response code [21] recently developed for the Elk branch of the original EXCITING FP-LAPW code [22], we derive low-energy effective models represented with the Wannier functions, the interaction parameters for which are evaluated by the constrained RPA.[13] To evaluate the AF coupling through the direct overlap between d orbitals, we first investigate a low-energy effective model for the Ru t_{2g} and O p bands in the energy window $[-7.0:+1.0]$ eV. We obtain the onsite Hubbard $U_d = 5.3$ eV and the largest transfer hopping between d orbitals $t_{dd} = 0.19$ eV, which result in a small AF coupling, $J \sim 4t_{dd}^2/U_d = 0.03$ eV.

We also derive an effective model only for the Ru t_{2g} bands in the energy window $[-1.4:+1.0]$ eV. In this model, the Wannier functions are the Ru t_{2g} orbitals hybridized with the surrounding O p orbitals, which allows a direct evaluation of the superexchange couplings. We obtain the on-site Hubbard $U = U(\mathbf{r} = 0) = 2.7$ eV,

the Hund's coupling $J_H = J(\mathbf{r} = 0) = 0.28$ eV, the nearest-neighbor off-site Coulomb interaction $V = 1.1$ eV, and the largest nearest-neighbor transfer hopping $= 0.28$ eV. For the AF superexchange coupling, these values result in $J_{AF} \sim 4t^2/(U - V) = 0.20$ eV. On the other hand, the F superexchange coupling J_F is evaluated as the nearest-neighbor off-site direct exchange ~ 0.03 eV. The superexchange AF coupling J_{AF} dominates over J and J_F . These estimates are replaced by an exact treatment in the following analysis.

In the atomic limit, each site has an $S = 3/2$ spin. When the two sites are coupled, the eigenstates can be labeled by the total spin $S = 0, 1, 2, 3$. Using the effective values of t , U , and J_H in the t_{2g} effective model [13], we perform exact diagonalization for two sites to obtain the energies of states labeled by S . These eigenvalues determine the exchange constants of a general effective spin-3/2 Hamiltonian for two sites as $H_{\text{eff}} = E_0 + J_1(\vec{S}_1 \cdot \vec{S}_2) + J_2(\vec{S}_1 \cdot \vec{S}_2)^2 + J_3(\vec{S}_1 \cdot \vec{S}_2)^3$. We find $J_1 = 45.6$ meV, $J_2 = -2.0$ meV, and $J_3 = 0.5$ meV. The interaction at the two site level is then primarily Heisenberg AF.

For purposes of modeling the system, we retain the Heisenberg AF nearest neighbor interactions within the plane (J_{\parallel} , 3 neighbors) taken as J_1 . Also, motivated by the experimental observation of G-type ordering, we introduce, in addition, a coupling between nearest neighbor planes (J_{\perp} , 2 neighbors). The classical Hamiltonian describing magnetism in SrRu_2O_6 is given by:

$$H_{\text{classical}} = J_{\parallel} \sum_{\langle ij \rangle_{\parallel}} \vec{S}_i \cdot \vec{S}_j + J_{\perp} \sum_{\langle ij \rangle_{\perp}} \vec{S}_i \cdot \vec{S}_j \quad (1)$$

For $J_{\perp} = 0$, according to the Mermin-Wagner theorem the long wave length spin waves destroy the long range order and consequently, the transition temperature tends to zero in the thermodynamic limit. However, a small inter-plane coupling can stabilize magnetic order. Our DFT calculations show that the inter-plane hopping parameters are small with respect to the in-plane parameters ($t_{\perp}/t_{\parallel} \sim 0.1$) which suggest that the AF inter-plane couplings J_{\perp} are between $0.1J_{\parallel}$ and $0.01J_{\parallel}$. We perform classical Monte Carlo simulations on a layered honeycomb lattice to obtain the transition temperature as a function of the ratio of these coupling constants. Figure 4 gives the results of these simulations for two values of J_{\perp}/J_{\parallel} .

The transition temperature obtained from Monte Carlo $T_N^{\text{MC}}(J_{\parallel}, J_{\perp})$ depends on the in-plane and inter-plane couplings in general as seen in Fig. 4. Using our estimated value for J_1 obtained from downfolding and exact diagonalization, we obtain the AF Heisenberg spin-3/2 coupling constant $J_{\parallel} = (3/2)^2 J_1 = 102.6$ meV or 1190 K. Further by using the experimental transition temperature of 565 K, we find that $J_{\perp} = 36$ K or equivalently $J_{\perp}/J_{\parallel} \approx 0.03$ fits the experimental results. The theoretical results also suggest that the transition tem-

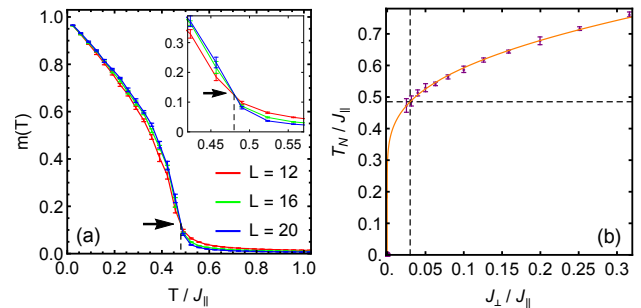


FIG. 4. (color online). (a) Classical Monte Carlo simulations using the model in (1) show the staggered magnetization per site versus temperature for $J_{\perp}/J_{\parallel} = 0.03$ using three system sizes of linear length L . The transition temperature $T_N = 0.48J_{\parallel}$ is obtained by locating the intersection of the curves with different system sizes. An enhanced plot near this point is given in the inset. Arrows point to the intersection point, and the corresponding transition temperature is indicated with dotted lines. (b) Transition temperature T_N in units of J_{\parallel} is plotted as a function of the ratio between the inter-plane and in-plane couplings. The horizontal dotted line shows the value of $T_N/J_{\parallel} = 0.48$ from comparing $T_N = 565$ K from experiment with $J_{\parallel} = 1190$ K from theory. A vertical dotted line shows the corresponding value of $J_{\perp}/J_{\parallel} = 0.03$. A fit to $J_{\parallel}/T_N = \alpha_1 + \alpha_2 \log J_{\parallel}/J_{\perp}$ from [23] using fitting parameters $\alpha_1 = 0.97$ and $\alpha_2 = 0.31$ is given as a solid line.

perature can be enhanced by increasing the in-plane coupling, for example by chemical or applied pressure.

As illustrated in the inset of Fig. 1, the quasi-two-dimensional crystal structure of SrRu_2O_6 distinguishes itself from other reported high T_c compounds with a perovskite structure. With the nonmagnetic Sr spacing layers the inter-plane coupling is expected to be weak. This is supported by our Monte Carlo simulations. The inter-plane coupling is small, but critical for the three dimensional magnetic order. The strong in-plane magnetic interaction is dominated by the AF superexchange coupling between rutheniums mediated by oxygen. We notice in Fig. 1 only one weak slope change around T_N and also the magnetic susceptibility increases linearly with increasing temperature above T_N . The absence of a Curie-Weiss-like paramagnetic behavior above T_N suggests that strong two dimensional magnetic fluctuations exist above T_N and persist until this compound decomposes around 800 K.

Our theoretical modeling highlights the mechanism for the high AF temperature. Similar to the mechanism for the perovskite SrTcO_3 in Ref. [2], we find that SrRu_2O_6 is close to the fluctuating regime with $U \sim W$ on the localized side. This is facilitated by substantial hybridization between Ru $4d$ and O $2p$ within the unit cell as seen from the projected density of states in Fig. 3(b) that reduces the effective U . In addition the hybridization between unit cells enhances the band width W , bringing this material close to the crossover region where T_N is enhanced.

Thus, the large covalency reduces the Ru moment but also facilitates a strong (in-plane) AF superexchange interaction important for the high T_N .

With multiple t_{2g} orbitals and Coulomb correlations that generate antiferromagnetism with high ordering temperatures on a honeycomb lattice, it is possible that this material has interesting topological properties that still need to be explored, especially as we replace Ru with the heavier Os and spin-orbit coupling becomes important. It could also be a parent material to explore the possibility of superconductivity upon doping at Sr and Ru sites or changing the oxygen nonstoichiometry. SrRu₂O₆, therefore, provides a new materials platform for studying the mechanism inducing high temperature magnetic order and other exotic phenomena in $4d$ and $5d$ transition metal oxides.

Work at ORNL was supported by the U.S. Department of Energy, Office of Science, Basic Energy Sciences, Materials Sciences and Engineering Division (synthesis and characterization) and Scientific User Facilities Division (neutron diffraction). The theoretical modeling (CS and NT) were supported by the CEM, and NSF MRSEC, under grant DMR-1420451. RA thanks a fruitful discussion with S. Sakai and Y. Nomura. JGC is supported by the National Basic Research Program of China (Grants No. 2014CB921500), the National Science Foundation of China (Grants No. 11304371), and the Strategic Priority Research Program (B) of the Chinese Academy of Sciences (Grants No. XDB07020100).

-
- [1] E. E. Rodriguez, F. Poineau, A. Llobet, B. J. Kennedy, M. Avdeev, G. J. Thorogood, M. L. Carter, R. Seshadri, D. J. Singh, and A. K. Cheetham, Phys. Rev. Lett. **106**, 067201 (2011)
 - [2] J. Mravlje, M. Aichhorn, and A. Georges, Phys. Rev. Lett. **108**, 197202 (2012)
 - [3] V. S. Borisov, I. V. Maznichenko, D. Bttcher, S. Ostanin, A. Ernst, J. Henk, and I. Mertig, Phys. Rev. B **85**, 134410 (2012)
 - [4] C. Franchini, T. Archer, Jianguang He, Xing-Qiu Chen, A. Filippetti, and S. Sanvito Phys. Rev. B **83**, 220402(R) (2011)
 - [5] S. Middey, Ashis Kumar Nandy, S. K. Pandey, Priya Mahadevan, and D. D. Sarma, Phys. Rev. B **86**, 104406 (2012)
 - [6] G. Thorogood, M. Avdeev, M. L. Carter, B. J. Kennedy,

- J. Ting, K. S. Wallwork, Dalton Transactions **40**, 7228 (2011)
- [7] O. Nganba Meetei, Onur Erten, Mohit Randeria, Nandini Trivedi, and Patrick Woodward Phys. Rev. Lett. **110**, 087203 (2013)
- [8] H. Kato, T. Okuda, Y. Okimoto, Y. Tomioka, Y. Takenoya, A. Ohkubo, M. Kawasaki and Y. Tokura, Appl. Phys. Lett. **81**, 328 (2002)
- [9] Y. Krockenberger, K. Mogare, M. Reehuis, M. Tovar, M. Jansen, G. Vaitheeswaran, V. Kanchana, F. Bultmark, A. Delin, F. Wilhelm, A. Rogalev, A. Winkler, and L. Alff, Phys. Rev. B **75**, 020404(R) (2007)
- [10] Y. G. Shi, Y. F. Guo, S. Yu, M. Arai, A. A. Belik, A. Sato, K. Yamaura, E. Takayama-Muromachi, H. F. Tian, H. X. Yang, J. Q. Li, T. Varga, J. F. Mitchell, and S. Okamoto, Phys. Rev. B **80**, 161104(R) (2009)
- [11] S. Calder, V. O. Garlea, D. F. McMorrow, M. D. Lumsden, M. B. Stone, J. C. Lang, J.-W. Kim, J. A. Schlueter, Y. G. Shi, K. Yamaura, Y. S. Sun, Y. Tsujimoto, and A. D. Christianson, Phys. Rev. Lett. **108**, 257209 (2012)
- [12] C. I. Hiley, M. R. Lees, J. M. Fisher, D. Thompsett, S. Agrestini, R. I. Smith, and R. I. Walton, Angew. Chem. Int. Ed. **53**, 4423 (2014)
- [13] See Supplementary Material for (1) experimental details, (2) refinement of the neutron diffraction pattern taken at 300 K, (3) temperature dependence of electrical resistivity, (4) Band structure and DOS for NM state.
- [14] R. M. Moon, T. Kiste, and W. C. Koehler, Phys. Rev. **181**, 920 (1969).
- [15] Q. Huang, P. Karen, V. L. Karen, A. Kjekshus, J. W. Lynn, A. D. Mighell, N. Rosov, and A. Santoro, Phys. Rev. B **45**, 9611 (1992).
- [16] J. W. Lynn, N. Rosov, and G. Fish, J. Appl. Phys. **73**, 5369 (1993).
- [17] J.B. Goodenough, Phys. Rev. **100** 564 (1955); J. Phys. Chem. Solids **6**, 287 (1958)
- [18] J. Kanamori, J. Phys. Chem. Solids **10** 87 (1959).
- [19] P. Blaha *et al.*, <http://www.wien2k.at>
- [20] J. P. Perdew and Y. Wang, Phys. Rev. B **45**, 13244 (1992).
- [21] A. Kozhevnikov *et al.*, in SCf10 Proceedings of the 2010 ACM/IEEE International Conference for High Performance Computing, Networking, Storage, and Analysis (IEEE Computer Society, Washington, DC,2010), pp. 1-10.
- [22] J. Spitaler *et al.*, The EXCITING FP-LAPW code: <http://exciting.sourceforge.net/>
- [23] K. Lee, Journal of Magnetism **6**(4), 119-121 (2001)
- [24] We call the Ru- d bands near the Fermi energy the “ t_{2g} ” bands for convenience whereas the t_{2g} bands experience an additional crystal field splitting in this material. However, it is just a unitary transformation of the basis in our model, and so does not affect the following analysis.